ELSEVIER

Seminars in
NUCLEAR
MEDICINE

Lung Scintigraphy in the Assessment of Aerosol Deposition and Clearance

Alejandro Sanchez-Crespo, MSc, PhD*,†

Environmental and occupational exposure to particulate aerosols is known to have negative health effects. However little is known about how these aerosols trigger the development of pathophysiological mechanisms in the body or the fate of ultrafine particles in the lungs after inhalation. The development of aerosols of different origin that can be labeled to a large variety with radionuclides compatible with clinical gamma camera systems opens the possibility of using lung scintigraphy imaging to study these causalities in detail. Lung scintigraphy (planar or SPECT) allows regional mapping of the deposition of the aerosol in the lungs and the dynamic assessment of particle clearance and translocation from the healthy and affected human lungs. In this paper, we will review the unique features of lung scintigraphy applied to aerosol clearance studies in humans.
Semin Nucl Med 49:47-57

Introduction

The lungs sustain life by promoting gas exchange in blood and acting as a barrier to foreign agents suspended in air like dust, fibers, and bacteria. While the process of gas exchange in the lungs is studied by school age children and has been investigated with radioactive tracers for over 50 years,[1] the protective function is still not well known by the general public. The lungs are the only internal organ directly exposed to external environment and air-suspended particulate matter pollutants (PM), ranging from micrometer (10^{-6} m) to nanometer (10^{-9} m) sizes. Exposure to PM has become common with the advent of industrialization and massive use of combustion engines, road transportation and every day commercial products containing aerosols. Nanoparticles, also denoted ultra-fine particles (UFPs), of sizes less than 0.1 microns, are the major constituent of man-made PM pollutants. These UFPs can accumulate in the most distal parts of the airways and alveoli from where they can potentially translocate to the systemic circulation. Hence, the health and environmental effects of these air-suspended PM pollutants of different origins (like metals, polycyclic aromatic hydrocarbons, carbon and other motor combustion related compounds as well as textile fibers, dust, and pollen) is the subject of increasing international concern (World Health Organization). Occupational exposure to PM in suspension of different sizes may be relevant for specific professions and in residential areas close to heavy industries and motorways. Elimination of these foreign agents occurs by trapping and mucus transport in the ciliated cells of the epithelium at the upper and lower airways in the lungs and by cellular pinocytosis and macrophage phagocytosis within the alveoli. However, how effective these processes are in relation to the particle size distribution and physicochemical characteristics in sick and healthy lungs is still not well understood. Further, little is known about the fate of UFP in the alveoli. It is plausible that UFP, due to the small size and large surface area per unit mass (capable of carrying large amounts of toxic materials or biological entities), can impair phagocytosis, initiate the release of inflammatory mediators and directly translocate into the systemic circulation via the alveolar-capillary membrane, from where they can further accumulate in the arteries or in secondary organs. These processes may contribute to the development of pathophysiological mechanisms in the body. International efforts are made to study in vivo the health effects and pathophysiological mechanism of exposure to UFP in the human body under controlled exposure conditions. Previous epidemiological and human studies have shown a direct association between exposure to UFP matter and atherosclerotic plaque expansion or rupture,[2-4]

*Department of Medical Radiation Physics and Nuclear Medicine, Karolinska University Hospital, Stockholm, Sweden.
†Department of Oncology-pathology. Karolinska Institutet, Stockholm, Sweden.
Address reprint requests to Alejandro Sanchez-Crespo, Department of Medical Radiation Physics and Nuclear Medicine, Karolinska University Hospital, Stockholm, Sweden. E-mail: alejandro.sanchez-crespo@sll.se

https://doi.org/10.1053/j.semnuclmed.2018.10.015
0001-2998/

thrombus formation,[5,6] the onset of oxidative stress and inflammatory process[7,8] and acute coronary events, especially among patients with underlying coronary artery disease.[9] The development of aerosols of different origin that can be label to a large variety of radionuclides, some of which are routinely used at nuclear medicine clinics, opened the possibility of using lung scintigraphy imaging to study in detail these causalities. Lung scintigraphy allows not only for in vivo mapping of the regional deposition of the aerosol in the lungs but also for longitudinal assessment of the clearance and translocation of aerosol particles from the healthy and affected human lungs. In this paper, we will review the unique features of lung scintigraphy applied to aerosol clearance studies in humans. The major aspects that will be covered are lung scintigraphy sensitivity at low radioactivity levels, measurements of radioactivity leaching from the aerosol particles (due to limited chemical stability of the bond), image quantification and radiation protection.

Properties of the Aerosolized Radionuclides for Lung Clearance Studies

The average adult human airway system can be divided in[10];

- the central or large airways; trachea, main bronchi, lobar bronchi, segmental bronchi, and subsegmental bronchi (mean diameter ranging from 1.8 to 0.186 cm)
- the peripheral or small airways; terminal bronchi and bronchioles (mean diameter ranging from 0.154 to 0.066 cm)
- the more distal or acimus; terminal bronchioles, respiratory bronchioles, and alveolar ducts alveolar sacs (ranging in mean diameter from 0.060 to 0.042 cm).

The degree of aerosol particle penetration in the human airway tree is therefore determined by the aerosol physical characteristics; particle size and distribution, shape, charge, density, and hygroscopicity.[11-13] PM_{10} (particulate matter with 10 micrometer diameters) or larger accumulates mainly in the large airways by inertial impaction. Smaller particles of the size of a few microns (like $PM_{2.5}$, particulate matter with 2.5 micrometer diameters) may penetrate deeper in the lungs and deposit in the distal airways walls by gravitational sedimentation. Finally, UFP (the major constituent of PM) may deposit and accumulate by Brownian diffusion in the most distal air spaces of the bronchioles and alveolar sacs.[14] Hence, the choice of aerosol generation method and material will determine which of these anatomical locations within the lungs can be reached and which elimination processes can be studied. If the goal of the assay is to study alveolar particle deposition and further translocation to secondary organs, radiolabeled particles of about 100 nanometers or smaller, should be used.[15-17] A wide range of aerosolized radionuclides have been used in human deposition and clearance assays (Table 1). The following is a summary of the most relevant.

Nebulized Radionuclides

A nebulizer can produce droplets from a solution of carrier (usually water or saline) mixed with a radionuclide via the Venturi effect. Particle size characteristics of the aerosol are largely determined by the design of the nebulizer and the driving gas flow employed. In routine clinical nuclear medicine, a saline solution containing diethylene-triamine pentaacetate labelled with ^{99m}Tc ([^{99m}Tc]DTPA) is routinely used for assessing alveolar epithelial membrane permeability damage.[18-22] Nebulizers, capable of aerosol generation with a median particle diameter as low as 2 μm were commercially available at the very beginning of the use of lung scintigraphy. Hence one of the early applications of [^{99m}Tc]DTPA was to measure lung penetration index and deposition.[23]

Technegas Aerosol Generator

Technegas aerosol is to date the most widely used ventilation agent in clinical nuclear medicine[24] and deserves special attention for longitudinal aerosol clearance studies. As a commercial product (Cyclomedica Ltd, Australia), the technegas generator produces an ultrafine suspension of carbon particles labeled with technetium-99 m (^{99m}Tc). The aerosol generation begins by evaporating to dry a solution of ^{99m}Tc-sodium pertechnetate ([^{99m}Tc]$NaTcO_4$) in a graphite crucible. Thereafter, in an argon atmosphere, an electric current is transmitted through the crucible for 15 s. The pertechnetate ion is then progressively reduced to metallic ^{99m}Tc as the temperature of the graphite crucible rises from room temperature to about 1000°C. Thereafter, at a crucible temperature of about 2550°C, the metallic ^{99m}Tc and the graphitic carbon are vaporized. The aerosol is then formed by first cocondensation of ^{99m}Tc and carbon vapors followed by agglomeration of airborne nanoparticles of ^{99m}Tc encapsulated in graphitic carbon.[25] This standard aerosol generation procedure results in UFP with a count median diameter (CMD) between 100 and 200 nm or even larger, due to high particle number concentration in the generator collection chamber and the rapid particle coagulation.[26,27] Modifications of the commercial technegas generator have been made to produce aerosols with smaller CMD by adding a timer-relay to the circuitry of the generator and changing the value of an internal potentiometer.[28,29] This allows control of the crucible evaporation time, which in turn modulates the CMD of the aerosol. With these modifications an aerosol with extremely small CMD of 35 nm, could be generated,[30] which remains the smallest CDM achieved with radiolabeled aerosols in human studies. Further modifications of the standard technegas generator operation are required to reduce the remaining fraction of salt in the crucible (from the ^{99m}Tc generator normal saline eluent) by an ion exchange column (Amberlite IR-120, MERCK, Germany). If not removed, this fraction of soluble saline may also evaporate and condense through the burning step, producing highly hygroscopic particles loosely bound to ^{99m}Tc. This free ^{99m}Tc, which may account for up to 12% of

Table 1 Summary of the Major Characteristics and Findings from Representative Retention Studies in Humans Using Radiolabel Aerosol

Reference	Volunteers	Aerosol (CMD)	Exposure	Detection Method (Sampling Time)	Activity Leaching Correction	Main Results
Wiebert 2006[16]	Healthy nonsmokers (n = 9) + asthmatics (n = 4)	99mTc-Technegas (35 nm)	Orally, deep breath followed by breath holding	GC (0-24 h) Ge (leaching)	From in vitro aerosol + whole blood and urine	100% lung retention. No difference between groups.
Wiebert 2006[30]	Healthy nonsmokers (n = 15)	99mTc-Technegas (100 nm)	Orally, deep breath followed by breath holding	GC (0-25 h) NaI (25.5-70 h) NaI (leaching)	From in vitro aerosol + whole blood and urine	99% lung retention
Klepczyńska-Nyström 2012[17]	Healthy nonsmokers (n = 9)	111In-Technegas (84 nm)	Orally, deep breath followed by breath holding	GC (0-168 h) NaI(leaching)	From in vitro aerosol + whole blood and urine	4.3 % particle clearance from lung but no translocation to secondary organs
Anderson 1995[37]	Healthy nonsmokers (n = 6)	111In-Teflon (6 μm)	Orally, extremely slow inhalation rate 0.04 L/s	NaI (0-96 h)	—	50% aerosol deposition. 35.4% aerosol retention in airways
Camner 1997[41]	Healthy nonsmokers (n = 6 $\times$ 3 groups)	111In-Teflon (6 μm, 8 μm and 10 μm)	Orally, extremely slow inhalation rate 0.05 L/s	NaI(0-72 h)	—	37.4%, 25% and 22% retention for the 6 μm, 8 μm and 10 μm, respectively
Ericsson 1995[40]	Smokers with chronic bronchitis (n = 14)	111In-Teflon (3.6 μm)	Orally, deep inhalations at a rate 0.5 L/s	NaI(0-72 h)	—	48% lung retention
Falk 1997[42]	Healthy nonsmokers (n = 8)	111In-Teflon (6.2 μm)	Orally, deep inh. (0.45 a 0.045 L/s	NaI(0-648 h)	In vitro leaching from particles in water	65% and 72% cleared from lungs for at 0.45 L/s and 0.045 L/s, respectively
Philipson 2000[13]	Healthy nonsmokers (n = 9)	111In-Polystirene (6.05 μm) 111In-Teflon (4.47 μm)	Orally, deep inhalations at 0.045 L/s.	NaI(0-24 h)	In vitro leaching from particles in water	51% and 47% lung retention for the polystyrene and Teflon aerosols, respectively
Philipson 1985[45]	Healthy nonsmokers (n = 6)	51Cr-Teflon (4 μm)	Orally, deep inhalations at 0.5 L/s	NaI(0-300d)	In vitro leaching from particles in water	49% lung retention
Philipson 1996[47]	Healthy smokers and nonsmokers (n = 10)	195Au-Teflon (3.6 μm)	Orally, deep inhalations at 0.5 L/s	NaI (0-900d) Ge (0-900d)	In vitro leaching from particles in water	Slow clearance (approx. 700 d biological half-times), with particle translocation to lymph nodes
Bennett 1998[48]	Healthy subjects (n = 11)	99mTc-iron oxide (3.5 μm)	Mouth shallow bolus inhalation at 50, 70 and 85% of TLC	GC (0-24 h)	—	DF ratio Left/Right 1.23, 1.6, and 1.96 for 50, 70, and 85% TLC About 30% retention for all boluses
Bennett 1999[49]	Healthy subjects (n = 16)	99mTc-iron oxide (6 μm)	Mouth shallow bolus inhalation at 70% of TLC	GC (0-24 h)	—	Variable intrathoracic airways DF among patients 27% retention

Table 1 (*Continued*)

Reference	Volunteers	Aerosol (CMD)	Exposure	Detection Method (Sampling Time)	Activity Leaching Correction	Main Results
Lindström 2005[39]	Cystic fibrosis patients (n = 11)	111In-Teflon (6 μm)	Orally, deep inhalations at 0.05 L/s.	NaI (0-21d)	—	Small airways deposition by sedimentation. Two phase clearance form lungs with larger retention in patients than in healthy subjects.
Lindström 2006[38]	Patients with primary ciliary dyskinesia (n = 6)	111In-Teflon (4.2 μm)	Orally, deep inhalations at 0.05 L/s.	NaI (0-21d)	—	Particle clearance continues in the small airways beyond 24 h. There are apparently additional clearance mechanisms present in the small airways
Lourenco 1971[52]	Healthy smokers (n = 9) and nonsmokers (n = 10)	198Au-iron oxide (2 μm)	Mouth, tidal volumes	GC(0-24 h)	—	Equal Tracheobronchial and alveolar deposition. 48% retention in non-smokers 47% retention in smokers
Meyer 2003[51]	Exsmokers with COPD (n = 10)	99mTc-iron oxide (3 μm)	Mouth, tidal volumes	NaI (0-24 h) GC (15 min)	—	Mean DF, 62% Peripheral and 16% bronchial
Möller 2008[29]	Healthy nonsmokers (n = 9), asymptomatic smokers (n = 10) and patients with COPD (n = 7)	99mTc-Technegas (100 nm)	Mouth, shallow boluses targeting conducting airways + deep boluses targeting alveoli	NaI (0-48 h) GC(45 min and 5 h)	From in-vitro aerosol + whole blood and urine	0.25% of inhaled aerosol deposited in the airways eliminated by mucociliary clearance. No clearance from periphery. No significant systemic particle translocation or accumulation of particles in the liver.
Phipps 1989[23]	Healthy volunteers (n = 7)	99mTc-DTPA (2.6-5.5 μm)	Mouth, tidal breathing	GC, SPECT and plannar imaging (after inhalation)	—-	SPECT derived PI is more relyable and accounts for more than 50% of inhaled aerosol.
Stahlhofen 1981[48]	Healthy nonsmokers (n = 5)	198Au-Teflon (4.7 μm) and 111In-Teflon (4.7 μm)	Mouth breathing tidal volume	NaI (0-160 h)	—	The long-term clearance rate following the short-term elimination of particles from ciliated airways was slower for Teflon particles (mean half-time 105 days for

Table 1 (Continued)

Reference	Volunteers	Aerosol (CMD)	Exposure	Detection Method (Sampling Time)	Activity Leaching Correction	Main Results
						111In-labeled particles and 128 days for 198Au-labeled particles)
Svartengren 2004[44]	Chronic bronchitis patients (n = 9) + age matched healthy (n = 15)	111In-Teflon (6 μm)	Orally, deep inhalations at 0.05 L/s	NaI (0-21d)	—	About 70% lung deposition. About 85% retention No difference in particle clearance between groups.
Falk 1999[46]	Healthy nonsmokers (n = 12)	51Cr-Teflon (6.1 μm)	Orally, at either 0.05 or 0.5 L/s	NaI (0-6 months)	—	Two-component exponential clearance with respectively 3.6 and 170 days half-times

COPD, Chronic obstructive pulmonary disorder; DF, Deposition fraction; DF, aerosol deposition fraction; GC, Gamma-camera; Ge, Germanium detectors; NaI, collimated-sodium-Iodine gamma counters; p.i., postinhalation; PI, Penetration Index = ratio of activity in a peripheral lung zone to a central lung zone; TLC, Total lung capacity.

the total generated gas,[29] rapidly clears from the lungs, which may jeopardize lung retention studies. Additionally, the presence of small amounts of oxygen during the burning step leads to the generation of so-called "pertechnegas",[31] which is rapidly cleared from the lungs. Figure 1, row-A and Figure 2 show the rapid pertechnegas clearance during the first hour post inhalation and the subsequent aerosol translocation to thyroid gland, stomach and intestines. For comparison Figure 1, row-B and Figure 2 show the corresponding deposition and slow clearance of low leaching 99mTc-Technegas UFP in a healthy individual at different time points.

Technetium-99m has a short physical half-life of 6 h, which in combination with the restricted amount of radioactivity that can be administered to humans in research studies and the limited sensitivity of gamma camera systems (due to the use of collimators), only permits short-term clearance studies. Another surrogate marker to label UF graphite particles in a technegas generator, more suitable for long-term clearance studies, is Indium-111.[29,32] Indium-111 (^{111}In) solution (2.8 days physical half-life) is obtained by evaporating to dryness a commercial indium chloride solution ([^{111}In]$InCl_3$, Amersham Braunschweig, Germany). This procedure is repeated by adding purified water until normal pH. Thereafter the remaining ^{111}In is dissolved in 99% ethanol as liquid carrier and inserted in the crucible of the technegas generator, running in pressurized air instead of argon to cause indium oxidation during the burning process ([^{111}In]In_2O_3). Indium oxide is insoluble in water and strongly bonds to graphite particles with a high chemical stability (low leaching). A study has shown that 7 days after generation, the cumulative radioactivity leaching reached about 5% of the initial radioactivity, for 50 nm CMD particles and merely 2% for 100 nm CMD particles.[32] This chemical stability allows for long-term follow-up of the deposition and retention of UFP aerosol. One recent study showed that the fate of inhaled 111In-labeled graphite UFP in humans can be accurately monitored during 1 month postinhaltation by combining the use of gamma camera planar imaging and high sensitive sodium iodine (NaI) scintillation detectors in a heavily shielded low background room[17]. Figure 1 row-C and Figure 2 illustrate the retention of 111In-Technegas during the first week post inhalation in a healthy individual.

Other interesting surrogate markers for technegas aerosol are isotopes of Gallium. Technegas labelled Gallium 68, also known as Galligas, has been reported in PET/CT ventilation studies.[33] The major advantage of Galligas is the possibility to exploit the fully tomographic and quantitative properties of PET/CT imaging. However the short physical half-life of Gallium 68 (68 minutes) precludes its use in long-term longitudinal clearance studies. For this purpose, technegas labelled Gallium 67 (3.3 days physical half-life), is more appropriate. Gallium 67 has gamma emission at 93, 184 and 300 keV, hence aerosol imaging sensitivity could be enhanced (even at low radioactive levels) by simultaneous imaging of these photon emission energies.

Teflon, Polystyrene and Iron Oxide Aerosols

A spinning disk machine atomizer[34] has been used in retention studies to generate monodispersed aerosols of different

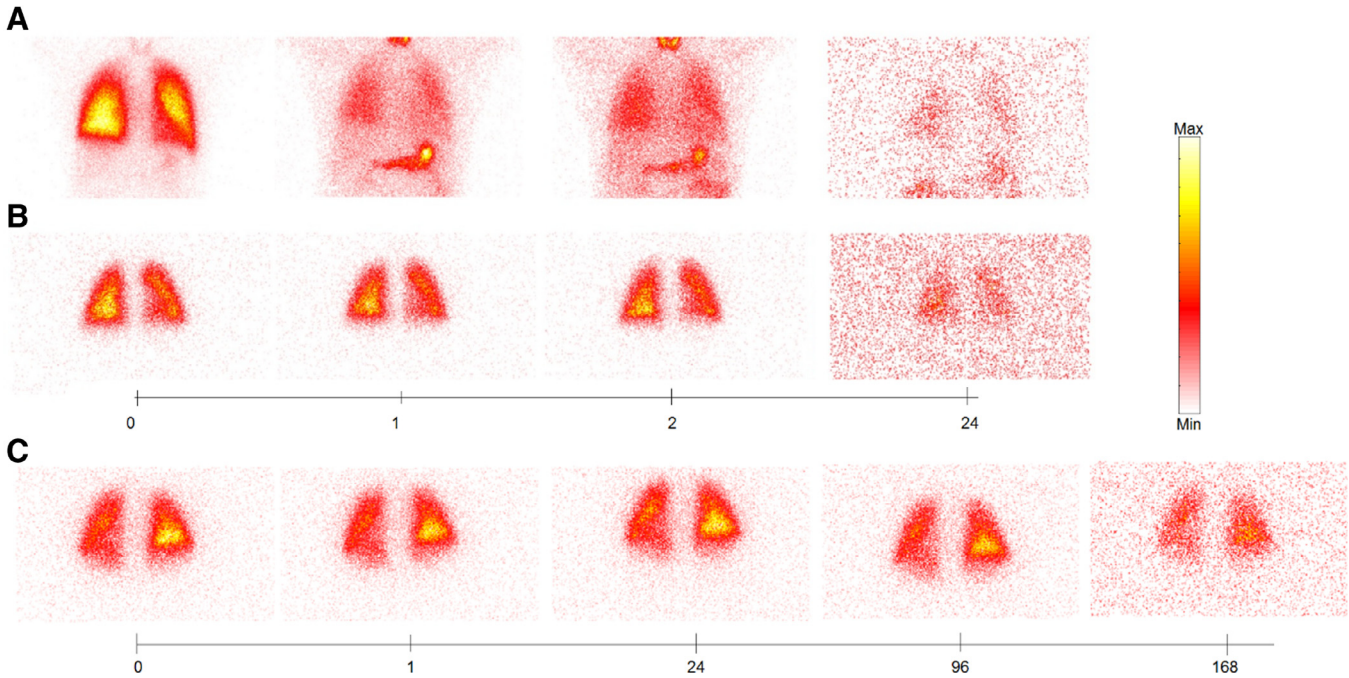

Figure 1 Gamma camera images after administration of an ultrafine particle aerosol labeled with 99mTc (rows A and B) and 111-In (row C). The images correspond to the geometric mean of the anterior and posterior lung scintigraphy at indicated time points (hours) postaerosol inhalation. Raw A, deposition of inhaled 99mTc-Technegas UFP aerosol mixed with large quantities of pertechnegas in a healthy subject. Raw B, the deposition of pure (no leaching) 99mTc-techneas UFP aerosol in a healthy volunteer with negligible clearance. Row C deposition and retention of 111In labeled technegas UFP aerosol in a healthy individual.

origin like Teflon, polystyrene materials and ferromagnetic iron oxide. These aerosols have been labeled with a number of different surrogate markers like technetium-99 m, indium-111, chromium-51, gold-195, and gold-198.[13,35-52]

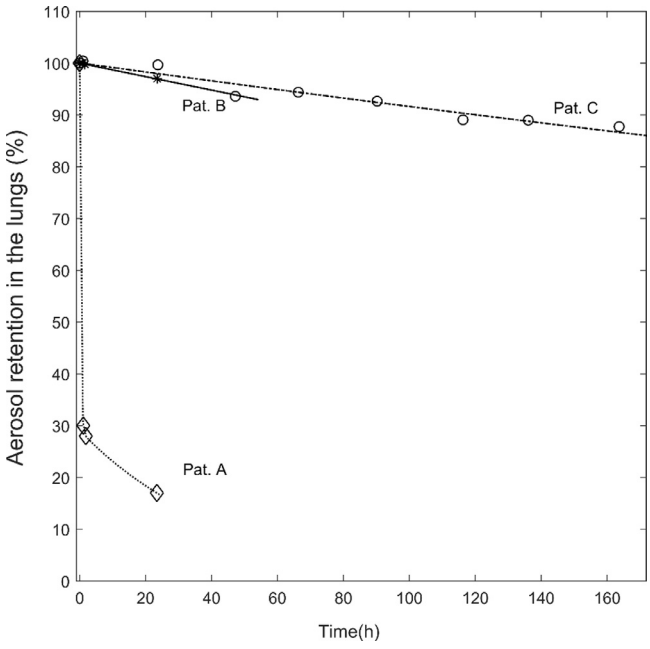

Figure 2 Time activity curves (TAC) for the patients displayed in Figure 1 and obtained from a region of interest around the lungs. Values are percentage of the initial inhaled activity.

Estimates of Radioactivity Leaching

In vivo measurements of the radiolabel-aerosol retention in the lungs with gamma camera imaging may be biased by the presence of free radioactivity leaching from aerosol particles. Correction for radioactivity leaching may be based on comparison with theoretical models of the aerosol deposition and clearance[53] or by in vitro longitudinal measurements of free radioactivity in samples of the inhaled aerosol and in samples of whole blood and urine, using the dialysis tube technique (Spectra/Pore, Spectrum Laboratories, Inc., Rancho Dominguez, CA) and a well-type NaI chamber. However, a drawback of this technique is the inability to discriminate leached radioactivity from the aerosol that is bond to blood proteins or other cells.

Biokinetic Monitoring of Radiolabeled Aerosols

As Table 1 reveals the combined use of lung scintigraphy and high sensitive gamma-counters, like sodium-iodine well-type chambers (NaI) or high purity Germanium detectors (HPGe), have been extensively used to map the regional distribution and biokinetic behavior of the radiolabeled aerosol in the body. In the previous section, we have briefly described radiolabeled aerosols of different origins. In this section, we will discuss how these radiolabeled aerosols are imaged using lung scintigraphy.

Initial Radioactivity and Radiation Doses

The accuracy in monitoring gamma emitters relies on good counting statistics. In gamma camera imaging, it is generally more reliable to measure large radioactivity quantities than a few Becquerel. However, exposure to ionizing radiation even at low doses heavily restricts the use of radioactivity in humans, since it carries a theoretical health risk. This risk is generally weighed against the benefits gathered from the study. The central assumption of a linear dose-response relationship for the induction of cancer, even at low doses, provides the basis for the calculation of maximum recommended radionuclide radioactivity for the assay.[54] This is a critical point requiring detailed consideration, since it determines which lung scintigraphy technique is suitable for imaging – planar or SPECT. Following, it is a practical example of the determination of the maximum administered radioactivity in terms of absorbed dose for ^{111}In-technegas aerosol (indigas) clearance studies. The absorbed radiation dose in the lungs per unit cumulated ^{111}In radioactivity in the lungs is [55];

$$S_{Lung \leftarrow Lung} = 3.78 \cdot 10^{-5} \left(\frac{Gy}{MBq \cdot h} \right) \quad (1)$$

Eq. (1) assumes homogeneously distributed source in the lungs. Assuming neither aerosol clearance from the lungs nor radioactivity leaching from the aerosol, the cumulative radioactivity in lungs is simply;

$$\overline{A}_{Lung} = \int_0^\infty A(t)dt = A_0 \int_0^\infty e^{-t}dt = \frac{A_0}{\lambda} \quad (2)$$

where A_0 is the initial inhaled radioactivity and $\lambda = \log_e(2)/68$ h. Finally, the absorbed dose to the lungs per unit administered radioactivity (MBq) is;

$$\begin{aligned} D_{Lung}(Gy) &= \overline{A}_{Lung} \cdot S_{Lung \leftarrow Lung} = 98.1 \text{ h}^{-1} A_0(MBq) \\ 3.78 \cdot 10^{-5} \left(\frac{Gy}{MBq \cdot h} \right) &= 0.0037 \left(\frac{Gy}{MBq} \right) \cdot A_0(MBq) \end{aligned} \quad (3)$$

For simplification, if the absorbed dose to the rest of the organs in the body is considered negligible, the associated effective dose is;

$$\begin{aligned} D(Sv) &= 0.0037 \left(\frac{Gy}{MBq} \right) \cdot A_0(MBq) \cdot H \cdot W_{Lung} \\ &= 0.0037 \cdot A_0 \cdot 1 \cdot 0.12 = 0.0004 \cdot A_0 \end{aligned} \quad (4)$$

where H and W_{Lung} are the radiation and tissue specific weighting factors. Hence, a 5 MBq indigas inhalation corresponds to an absorbed dose to the lungs of about 2 mSv. In terms of potential harm, this absorbed radiation dose is coupled to a lifetime risk to develop a fatal cancer of approximately 1 in ten thousand.[54] This risk is justifiable in basic science research with healthy individuals by setting an age threshold to the inclusion criteria.

At this level of initial inhaled radioactivity, 2-dimensional dynamic lung scintigraphy could be used to assess the kinetics of aerosol in the body for at least 2-3 physical half-lives of the radionuclide (in this case approximately 7 days postinhalation), thereafter aerosol monitoring can be continued for at least one more month with high sensitive gamma-counters (like NaI or HPGe detectors) in a room properly shielded from background radiation.

Lung Scintigraphy Imaging in Radiolabeled-Aerosol Assays

Dynamic 2-dimensional "planar" gamma-camera imaging (acquired in list-mode or sequentially with a given acquisition time interval), as well as three-dimensional single photon emission computed tomography (SPECT) can be used to map the regional distribution and the kinetics of the aerosol in the human lungs and in other anatomical localizations of the body.[56-59] Planar imaging is a well-established imaging technique for this application at low radioactivity levels. SPECT scanning, on the other hand, requires much higher radioactivity and longer scanning times, typically 15-20 minutes, (depending on the number of detector heads and the angular sampling) to achieve a good contrast to noise ratio (CNR);

$$CNR = \frac{C_O - C_B}{\sigma_B} \quad (5)$$

where C_O and C_B are the average count rate in a region of interest of the object and the background, respectively and σ_B the standard deviation in the background. The CNR in gamma camera imaging is coupled with the limited system sensitivity of the gamma camera (which basically depends on the collimator characteristics and the photon emission energy), the amount of radioactivity and the level of background radiation. The CNR may therefore substantially decrease, due to radioactive decay, aerosol clearance, and radioactivity leaching throughout the aerosol following up sequence. When the CNR of the object in gamma-camera image is below three, image quantification is very inaccurate[60,61] and hence the follow-up process should switch to more sensitive radiation detector devices. The variation of CNR for the intended image acquisition protocol and radionuclide radioactivity should be characterized with a phantom study prior the beginning of the human assay. A known radioactivity (corresponding to the intended administered radioactivity in the human study) is homogeneously distributed in the lungs cavities of a chest phantom or a cylindrical phantom and imaged through several physical half-lives. The CNR is then calculated according to Eq. (5) as a function of decay time. As an example, Figure 3 shows the variation in CNR for a thoracic phantom (Data Spectrum Inc., Chapel Hill, NC) uniformly filled with ^{111}In, to a concentration of 500 Bq/ml. The phantom was then placed in a two-headed gamma camera system (Trionix Research Laboratories, Twinsburg, OH) equipped with medium energy parallel-hole collimators. The image acquisition protocol was performed as previously described.[32] As Figure 3 reveals, 7 days after the beginning of the assay, the CNR dropped below the Rose[61] criterion for the specific settings of the measurement.

Lung Scintigraphy Analysis

Figure 4 shows the major differences in image acquisition and quantification between planar imaging and SPECT. Regional

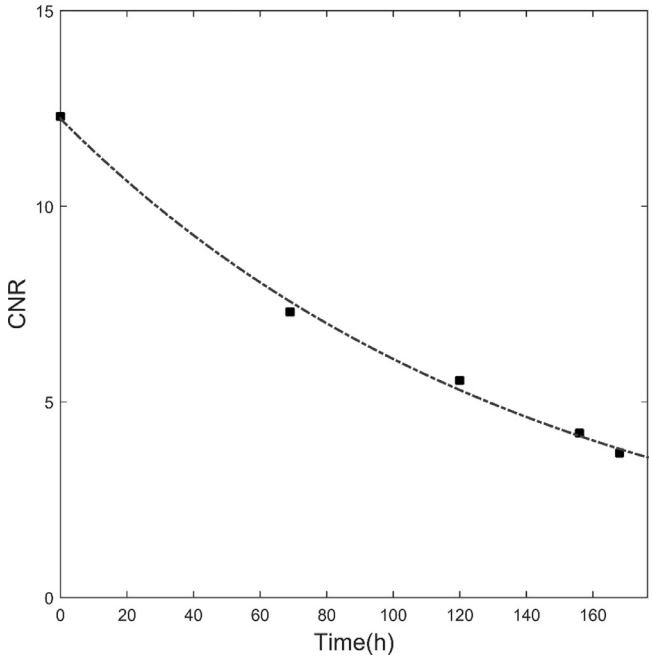

Figure 3 Relation between activity and contrast to noise ratio (CNR) obtained from a phantom study with initially 1 MBq 111-In activity diluted in the lungs cavities of a thorax phantom.

aerosol quantification in planar imaging is approximative because of the superposition of radioactivity in the direction of the projection. However, the total lung aerosol radioactivity and the corresponding relative rate of change after aerosol administration can be accurately determined using planar scintigraphy. The later can be obtained from time series of geometric mean attenuation corrected images (GM) of the anterior (A) and posterior (P) views of the lungs (background and decay corrected). For a point source located at a certain depth, assuming uniform attenuation, the GM will then be equal to;

$$GM = \sqrt{A \cdot P} = \sqrt{A_{air} e^{-\mu d} \cdot A_{air} e^{-\mu(T-d)}} = \sqrt{A_{air}^2 \cdot e^{-\mu T}} = A_{air} \cdot e^{-\frac{\mu T}{2}} \quad (6)$$

where A_{air} is the true radioactivity in the point without attenuation, d is the distance from the point source to the surface along the projection line toward one detector, T is the total patient thickness and μ is the linear attenuation coefficient. T and μ can be measured experimentally using a 57-Cobalt flood source:

$$C_p = C_{air} \cdot \exp(-\mu T) \quad (7)$$

where C_p and C_{air} are the count rate obtained with and without the patient between the cobalt source and the detector, respectively.[62] Finally A_{air} can be obtained combining Eqs. (6) and (7);

$$GM = A_{air} \cdot \exp\left(-\frac{\mu T}{2}\right) = A_{air} \cdot \sqrt{C_p/C_{air}} \cdot \text{From where } A_{air} = GM \cdot \sqrt{\left[\frac{C_{air}}{C_p}\right]^f} \quad (9)$$

Where a correction factor "f" has been added to Eq. (9) to account for the differences in water between the mass

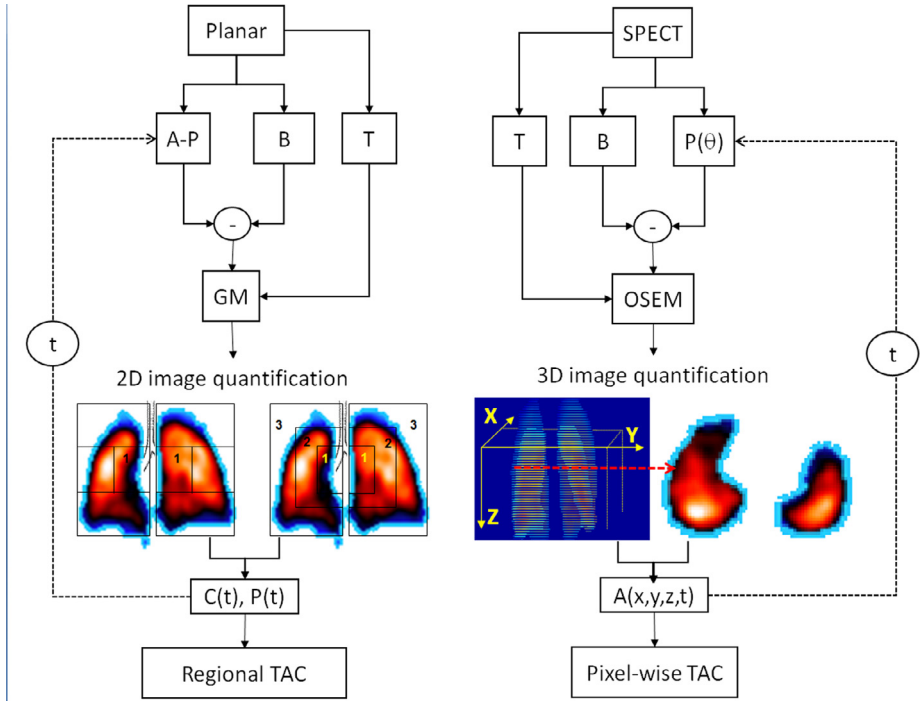

Figure 4 Overview of the lung scintigraphyc image acquisition and processing techniques for aerosol deposition and clearance studies in 2D (planar) and 3D (SPECT). A, activityl; A-P, anterior-posterior images; B, radiation background image; C, central lung region; GM, pixel wise geometric mean operation; OSEM: ordered subset expectation maximization reconstruction algorithm; P, peripheral lung region; P(θ): Gamma camera projection at angle θ; TAC, time activity curve; t, time; T, transmission image. Lung region 1.

attenuation coefficients for cobalt-57 (E_γ = 122 keV, $t_{1/2}$ = 272 days) and the radionuclide used to label the aerosol, $f = \mu/\mu_{Co}$. Regional quantification of the GM image as described in Figure 4 is carried out by defining the central (C) and peripheral (P) lung regions, corresponding to the large airways and the middle-distal airways. The lungs are divided in three equal regions of interest from where "central" is defined as half of the middle region closest to the hilum and "peripheral" the rest of the lung.[17,32] Other authors divide the GM image in three concentric onion-like layers, corresponding to the large, medium and small airways.[63] Time-activity curves (TACs), obtained by radioactivity quantification of the GM time series using the same regions of interest definition across time points represent the regional aerosol retention, from where the biological half-life can be calculated by least square fitting to an exponential equation (with one or several clearance phases). Radioactivity leaching correction at every point of the TAC may be applied from in vitro measurements of free radioactivity leaching from a sample of the inhaled aerosol in water. The same methodology can be applied to other anatomical localizations, like the liver, for visual and quantitative evidence of translocated aerosol. Figure 4 also shows the analysis and quantification of SPECT images. The major difference is the three-dimensional nature of the reconstructed images, allowing for a regional or pixel wise calculation of TACs.[23,58,64]

Gamma-Counters in Radiolabeled-Aerosol Assays

As previously described, the limited sensitivity in gamma-camera imaging, restricts their use only above a certain radioactivity level. Hence in long-term studies of the clearance of inhaled aerosols, gamma-camera imaging is combined with high sensitive gamma-counters, like large area sodium-iodine (NaI) and high-purity germanium (HPGe) detectors, placed in a low background level room and shielded well-chamber type NaI detectors. The detection efficiency of these gamma-counters is, for the photon energy range used in nuclear medicine, very high. Thus, the detector signal is susceptible to fluctuations even at small geometrical variations of the same sample. Hence, assays with these detectors require very good geometrical reproducibility. Additionally, for gamma-counters with more than one detector (like well-type chambers), a normalization of the different detectors counting efficiency (for the radionuclide of choice) is required. Finally, the detector settings, in terms of the size and position of the detection energy window, the type of background and decay correction, should be carefully set prior the start of the assay and kept unchanged though out the study. This setup determines the minimum detectable radioactivity of the assay and the maximum radioactivity levels of the sample above

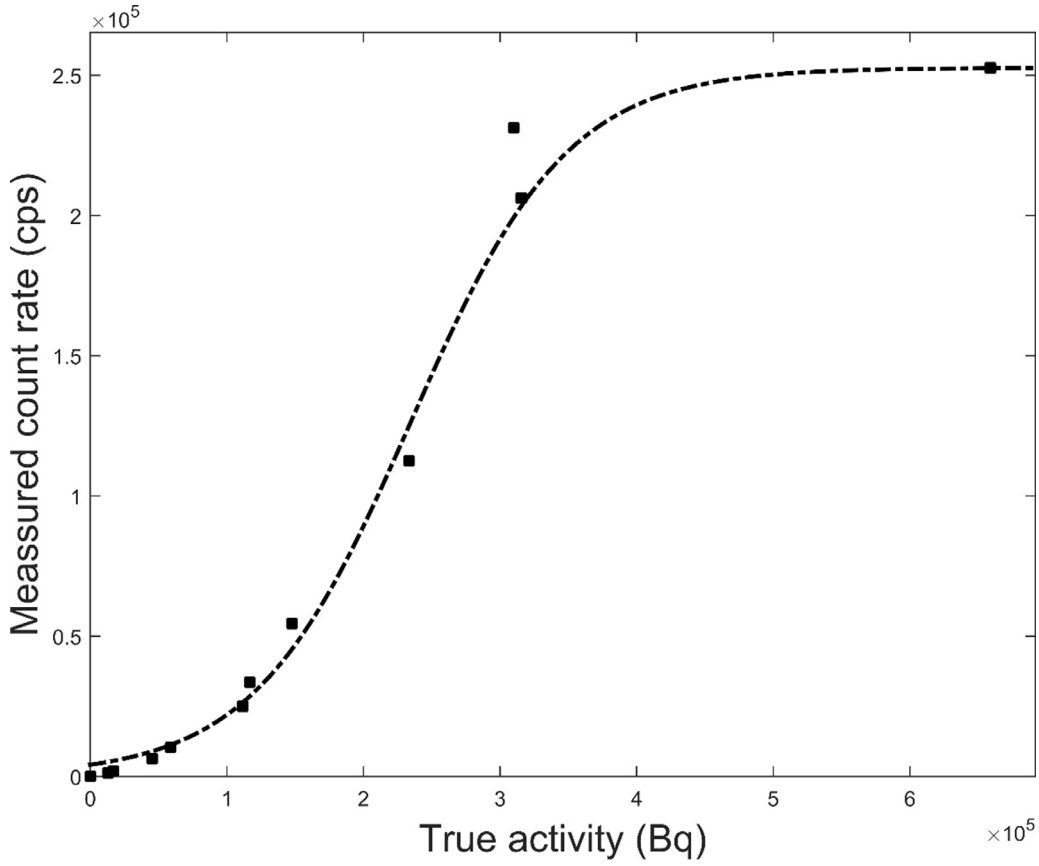

Figure 5 The characteristics response of a commonly use well-type NaI chamber as a function of activity concentration.

which counting losses, due to detector dead time, are significant. Figure 5 shows the response of a well-type NaI chamber to different radioactivity levels in a 1 ml sample containing ^{111}In. In this particular example, above 300 kBq/ml the radioactivity measurements are heavily hampered by count losses due to detector dead time. On the other hand, detector response is fairly linear down to 15 Bq/ml. Such low detection limits allow monitoring small amounts of radiolabeled aerosols in the order of picograms.

Conclusions

Lung scintigraphy is a well-established in vivo, noninvasive technique to investigate the fate of inhaled aerosols of different origin. This technique has revealed evidence of prolonged airway retention of nano and micro sized aerosol particles of different origin with very limited translocation towards the systemic circulation and secondary organs in healthy-nonsmokers (Table 1). We may speculate that this enhanced lung particle retention is caused by the ability of the extremely small particles to cross the mucous barrier and deposit directly on the inner surface of the small airways, impairing mucociliary transport. Further, particle elimination by interaction with macrophages in the most distal airways and alveolar sacs may also be inhibited or it may be too inefficient to be able to be monitored with the current nuclear medicine techniques.

References

1. West JB, Dollery CT: Distribution of blood flow and ventilation-perfusion ratio in the lung, measured with radioactive carbon dioxide. J Appl Physiol 15:405-410, 1960
2. Sun Q, Wang A, Jin X, et al: Long-term air pollution exposure and acceleration of atherosclerosis and vascular inflammation in an animal model. JAMA 294:3003-3010, 2005
3. Hoffmann B, Moebus S, Möhlenkamp S, et al: Residential exposure to traffic is associated with coronary atherosclerosis. Circulation 116:489-496, 2007. Epub 2007 Jul 16
4. Künzli N, Jerrett M, Mack WJ, et al: Ambient air pollution and atherosclerosis in Los Angeles. Environ Health Perspect 113:201-206, 2005
5. Peters A, Döring A, Wichmann HE, Koenig W: Increased plasma viscosity during an air pollution episode: A link to mortality? Lancet 349:1582-1587, 1997
6. Baccarelli A, Martinelli I, Zanobetti A, et al: Exposure to particulate air pollution and risk of deep vein thrombosis. Arch Intern Med 168:920-927, 2008
7. Gilmour PS, Brown DM, Beswick PH, et al: Free radical activity of industrial fibers: Role of iron in oxidative stress and activation of transcription factors. Environ Health Perspect 105(Suppl 5):1313-1317, 1997
8. Monteiller C, Tran L, MacNee W, et al: The pro-inflammatory effects of low-toxicity low-solubility particles, nanoparticles and fine particles, on epithelial cells in vitro: The role of surface area. Occup Environ Med 64:609-615, 2007
9. Rich DQ, Schwartz J, Mittleman MA, et al: Association of short-term ambient air pollution concentrations and ventricular arrhythmias. Am J Epidemiol 161:1123-1132, 2005
10. Weibel ER: Morphometry of the Human Lung. Berlin/New York: Springer-Verlag, 1963
11. Geiser M, Kreyling WG: Deposition and biokinetics of inhaled nanoparticles. Part Fibre Toxicol 7:2, 2010. https://doi.org/10.1186/1743-8977-7-2
12. Kreyling WG, Semmler-Behnke M, Takenaka S, et al: Differences in the biokinetics of inhaled nano- versus micrometer-sized particles. Acc Chem Res 46:714-722, 2013
13. Philipson K, Falk R, Svartengren M, et al: Does lung retention of inhaled particles depend on their geometric diameter? Exp Lung Res 26:437-455, 2000
14. Carvalho TC, Peters JI, Williams RO 3rd: Influence of particle size on regional lung deposition—What evidence is there? Int J Pharm 406:1-10, 2011
15. Oberdörster G, Sharp Z, Atudorei V, et al: Translocation of inhaled ultrafine particles to the brain. Inhal Toxicol 16:437-445, 2004
16. Wiebert P, Sanchez-Crespo A, Seitz J, et al: Negligible clearance of ultrafine particles retained in healthy and affected human lungs. Eur Respir J 28:286-290, 2006
17. Klepczyńska-Nyström A, Sanchez-Crespo A, Andersson M, et al: The pulmonary deposition and retention of indium-111 labeled ultrafine carbon particles in healthy individuals. Inhal Toxicol 24:645-651, 2012
18. Okudan B, Han S, Baldemir M, et al: Detection of alveolar epithelial injury by 99mTC-DTPA radioaerosol inhalation lung scan following blunt chest trauma. Ann Nucl Med 18:573-577, 2004
19. Suskind H: Technetium-99m-DTPA aerosol to measure alveolar-capillary membrane permeability. J Nucl Med 35:207-209, 1994
20. Caner B, Ugur O, Bayraktar M, et al: Impaired lung epithelial permeability in diabetics detected by technetium-99m-DTPA aerosol scintigraphy. J Nucl Med 35:204-206, 1994
21. O'Brodovich H, Coates G: Pulmonary clearance of 99mTc-DTPA: A noninvasive assessment of epithelial integrity. Lung 165:1-16, 1987
22. Durand E, Prigent A: The basics of renal imaging and function studies. Q J Nucl Med 46:249-267, 2002
23. Phipps PR, Gonda I, Bailey DL, et al: Comparisons of planar and tomographic gamma scintigraphy to measure the penetration index of inhaled aerosols. Am Rev Respir Dis 139:1516-1523, 1989
24. Burch WM, Sullivan PJ, McLaren C: Technegas — A new ventilation agent for lung scanning. Nucl Med Commun 7:865-871, 1986
25. Senden TJ, Moock KH, Gerald JF, et al: The physical chemical nature of Technegas. J Nucl Med 38:1327-1333, 1997
26. Lemb M, Oei TH, Eifert H, et al: Technegas: A study of particle structure, size and distribution. Eur J Nucl Med 20:576-579, 1993
27. Lloyd JJ, Shields RA, Taylor CJ, et al: Technegas and Pertechnegas particle size distribution. Eur J Nucl Med 22:473-476, 1995
28. Möller W, Felten K, Seitz J, et al: A generator for the production of radiolabelled ultrafine carbonaceous particles for deposition and clearance studies in the respiratory tract. J Aerosol Sci 37:631-644, 2006
29. Möller W, Felten K, Sommerer K, et al: Deposition, retention, and translocation of ultrafine particles from the central airways and lung periphery. Am J Respir Crit Care Med 177:426-432, 2008
30. Wiebert P, Sanchez-Crespo A, Falk R, et al: No significant translocation of inhaled 35-nm carbon particles to the circulation in humans. Inhal Toxicol 18:741-747, 2006
31. Mackey DW, Jackson P, Baker RJ, et al: Physical properties and use of pertechnegas as a ventilation agent. J Nucl Med. 38:163-167, 1997
32. Sanchez-Crespo A, Klepczynska-Nyström A, Lundin A, et al: ^{111} Indium-labeled ultrafine carbon particles; a novel aerosol for pulmonary deposition and retention studies. Inhal Toxicol 23:121-128, 2011
33. Borges JB, Velikyan I, Långström B, et al: Ventilation distribution studies comparing Technegas and "Gallgas" using 68GaCl3 as the label. J Nucl Med 52:206-209, Feb 2011
34. Camner P: The production and use of test aerosols for studies of human tracheobronchial clearance. Environ Physiol Biochem 1:137-154, 1971
35. Scheuch G, Philipson K, Falk R, et al: Retention of particles inhaled in boli with and without induced bronchoconstriction. Exp Lung Res 21:901-916, 1995
36. Scheuch G, Kreyling W, Haas F, et al: The clearance of polystyrene particles from human intrathoracic airways. J Aerosol Med 6(suppl):47, 1993
37. Anderson M, Philipson K, Svartengren M, et al: Human deposition and clearance of 6-micron particles inhaled with an extremely low flow rate. Exp Lung Res 21:187-195, 1995

38. Lindström M, Falk R, Hjelte L, et al: Long-term clearance from small airways in subjects with ciliary dysfunction. Respir Res 7:79, 2006
39. Lindström M, Camner P, Falk R, et al: Long-term clearance from small airways in patients with cystic fibrosis. Eur Respir J 25:317-323, 2005
40. Ericsson CH, Svartengren K, Svartengren M, et al: Repeatability of airway deposition and tracheobronchial clearance rate over three days in chronic bronchitis. Eur Respir J 8:18861-18893, 1995
41. Camner P, Anderson M, Philipson K, et al: Human bronchiolar deposition and retention of 6-, 8- and 10-micrograms particles. Exp Lung Res 23:517-535, 1997
42. Falk R, Philipson K, Svartengren M, et al: Clearance of particles from small ciliated airways. Exp Lung Res 23:495-515, 1997
43. Svartengren K, Philipson K, Svartengren M, et al: Tracheobronchial deposition and clearance in small airways in asthmatic subjects. Eur Respir J 9:1123-1129, 1996
44. Svartengren M, Svartengren K, Europe E, et al: Long-term clearance from small airways in patients with chronic bronchitis: Experimental and theoretical data. Exp Lung Res 30:333-353, 2004
45. Philipson K, Falk R, Camner P: Long-term lung clearance in humans studied with Teflon particles labeled with chromium-51. Exp Lung Res 9:31-42, 1985
46. Falk R, Philipson K, Svartengren M, et al: Assessment of long-term bronchiolar clearance of particles from measurements of lung retention and theoretical estimates of regional deposition. Exp Lung Res 25:495-516, 1999
47. Philipson K, Falk R, Gustafsson J, et al: Long-term lung clearance of 195Au-labeled teflon particles in humans. Exp Lung Res 22:65-83, 1996
48. Stahlhofen W, Gebhart J, Heyder J, et al: Intercomparison of regional deposition of aerosol particles in the human respiratory tract and their long-term elimination. Exp Lung Res 2:131-139, 1981
49. Bennett WD, Scheuch G, Zeman KL, et al: Regional deposition and retention of particles in shallow, inhaled boluses: Effect of lung volume. J Appl Physiol 86:168-173, 1999
50. Bennett WD, Scheuch G, Zeman KL, et al: J Appl Physiol 85:685-694, 1998
51. Meyer T, Müllinger B, Sommerer K, et al: Pulmonary deposition of monodisperse aerosols in patients with chronic obstructive pulmonary disease. Exp Lung Res 29:475-484, 2003
52. Lourenço RV, Klimek MF, Borowski CJ: Deposition and clearance of 2 micron particles in the tracheobronchial tree of normal subjects—Smokers and nonsmokers. J Clin Invest 50:1411-1420, 1971
53. Finlay WH, Stapleton KW, Chan HK, et al: Regional deposition of inhaled hygroscopic aerosols: In vivo SPECT compared with mathematical modeling. J Appl Physiol (1985) 81:374-383, 1996
54. The 2007 Recommendations of the International Commission on Radiological Protection. ICRP publication 103. Ann ICRP. 37:1-332, 2007
55. Snyder WS, Ford MR, Warner GG, et al: "S" Absorbed Dose Per Unit Cumulated Radioactivity for Selected Radionuclides and Organs. MIRD Pamphlet No. 11. New York, NY: Society of Nuclear Medicine, 1975
56. Eberl S, Chan HK, Daviskas E: SPECT imaging for radioaerosol deposition and clearance studies. J Aerosol Med 19:8-20, 2006 Spring. Review
57. Eberl S, Chan HK, Daviskas E, et al: Aerosol deposition and clearance measurement: A novel technique using dynamic SPET. Eur J Nucl Med 28:1365-1372, 2001
58. Fleming J, Bailey DL, Chan HK, et al: Standardization of techniques for using single-photon emission computed tomography (SPECT) for aerosol deposition assessment of orally inhaled products. J Aerosol Med Pulm Drug Deliv 25(Suppl 1):S29-S51, 2012
59. Chan HK: Use of single photon emission computed tomography in aerosol studies. J Aerosol Med 6:23-36, 1993 Spring. Review
60. Sanchez-Crespo A, Jussing E, Björklund A-C, et al: Hallmarks in prostate cancer imaging with Ga68-PSMA-11-PET/CT with reference to detection limits and quantitative properties. EJNMMI Res 8:27, 2018
61. Rose A: Vision: Human and Electronic. New York: Plenum Press, 21-23, 1973
62. Macey D, Marshall R: Absolute quantitation of radiotracer uptake in lungs using a gamma camera. J Nucl Med 23:731-735, 1984
63. Newman SP, Wilding IR: Imaging techniques for assessing drug delivery in man. Pharm. Sci. Technol. Today 2:181-189, 1999
64. Logus JW, Trajan M, Hooper HR, et al: Single photon emission tomography of lungs imaged with 99mTc-labeled aerosol. J Can Assoc Radiol 35:133-138, 1984